Water Adsorption and Desorption Isotherms of Silica and Alumina Mesoporous Molecular Sieves

SRIDHAR KOMARNENI, RAJYALAKSHMI PIDUGU AND VINAYAN C. MENON
Intercollege Materials Research Laboratory, The Pennsylvania State University, University Park, PA 16802

Abstract. Mesoporous molecular sieves of silica, and alumina, and porous materials of titania, zirconia, and niobia were synthesized by cationic and/or neutral templating methods. These porous materials were characterized by powder X-ray diffraction, transmission electron microscopy, N_2 adsorption-desorption isotherms and water adsorption-desorption isotherms. Mesoporous molecular sieves of silica with surface areas of 956 and 1072 m^2/g and of alumina with surface area of 407 m^2/g were synthesized. The Ti, Zr and Nb oxide porous materials, however, showed smaller surface areas of 258, 178, and 77 m^2/g, respectively, after calcination at 300°C and exhibited only small peaks for mesopores as determined by the pore-size distributions.

Water adsorption-desorption isotherms of silica and alumina mesoporous molecular sieves showed Type V (weak interaction) and Type IV isotherms, respectively. The property of sudden filling of mesopores in the P/P_0 range of 0.45 to 0.55 in silica mesoporous molecular sieves with well-defined hysteresis during desorption, can be used in the design of humidity sensors. The titania, zirconia and niobia porous materials showed Type I water adsorption-desorption isotherms which suggests that these are mainly microporous. These results suggest that water adsorption-desorption isotherms provide valuable information about mesoporous molecular sieves for their potential use as humidity sensors.

Keywords: mesoporous molecular sieves, water adsorption-desorption, cationic template, neutral template, mesoporous silica molecular sieve, mesoporous alumina molecular sieve, humidity sensor, mesoporous materials

1. Introduction

Two new types of mesoporous materials with well-defined unimodal pore-size distribution have been reported starting in 1990 [1–3]. Mesoporous silicates were first reported by Yanagisawa et al. [1]. These materials with uniform pore-size were prepared by intercalation of kanemite, a layered silicate with alkyltrimethylammonium ions and subsequent calcination at 700°C or higher temperatures. Researchers from Mobil Corporation discovered a new family of mesoporous molecular sieves with tailored pore-sizes in the range of 1.5 to 10 nm and their results were published in 1992 [2, 3]. The synthesis of these mesoporous silicates and aluminosilicates was accomplished by hydrothermal treatment of silica and aluminosilicate precursors in the presence of quaternary ammonium salts such as cetyltrimethylammonium chloride or dodecyltrimethyl-ammonium chloride. In these syntheses, the cationic surfactant molecules form a micelle/liquid-crystal phase that serve as templates on which the anionic inorganic silica or aluminosilicate condenses [2, 3], i.e., electrostatic assembly. Porosity is created by removing the organic templates. The breakthrough in the design and synthesis of mesoporous materials was followed by a flurry of activity by several researchers because of their obvious importance in catalysis, molecular sieving, etc. The electrostatic assembly [2, 3] of these mesoporous materials has been thoroughly documented [4–7]. Tanev and Pinnavaia [8, 9], however, recently demonstrated a neutral templating route for preparing mesoporous

molecular sieves based on hydrogen-bonding inter-actions and self-assembly between neutral primary amine micelles and neutral inorganic precursors. This new synthesis strategy not only extended the range of chemical compositions from which mesoporous materials can be synthesized, but also led to the facile, environmentally-benign recovery of the template by simple extraction [8]. In addition to the above important contribution, the Michigan State group led by Pinnavaia reported very recently [10] the synthesis of mesoporous molecular sieves from the hydrolysis of metal alkoxides in the presence of nonionic polyethylene oxide surfactants which are low-cost, nontoxic and biodegradable. The synthesis and characterization studies are being followed up by catalytic studies [11–13] using these materials. A thorough characterization and property evaluation of these materials is of paramount importance in their eventual application in different fields. Here we report the synthesis, characterization and water adsorption-desportion properties of some mesoporous materials. The water adsorption-desorption properties reveal the polarity of their surfaces, i.e., hydrophilic or hydrophobic nature which is an important property for several applications. The water adsorption-desorption isotherms are also important in designing humidity sensors. Water adsorption properties of MCM-41 type mesoporous materials were reported previously by others [14–16].

2. Experimental

Mesoporous materials were prepared by two previously described methods [3, 8, 9]. A mesoporous silica sample was prepared by the method of Beck et al. [3] as follows: 20 g of water, 9.48 g of sodium silicate (28.3% silica) and 0.6 g of sulfuric acid were mixed and stirred for 10 minutes in the Teflon cup of a Parr bomb. To this mixture, 8.385 g of cetyltrimethyl ammonium bromide dissolved in 25.115 g of deionized water was added which yielded a gel. The gel mixture was stirred for 30 minutes and then 10 g of deionized water was added. The mixture was sealed in the Parr bomb which was then heated in a drying oven at 100°C for 144 hours. After the above hydrothermal treatment, the solid and solution phases were separated by centrifugation. The solid phase was repeatedly washed with deionized water and dried at 60°C. This sample was calcined at 300°C for 25 hours to remove the entrapped cetyltrimethyl ammonium cation before N_2 and H_2O adsorption measurements.

Mesoporous materials of silica, alumina, titania, zirconia and niobia were prepared using tetraethoxysilane, Al isopropoxide, Ti isopropoxide, Zr butoxide and Nb ethoxide, respectively by the method of Tanev and Pinnavaia [8, 9]. This method uses a neutral templating route in the preparation of mesoporous material unlike the cationic template route [3] described above. The general procedure used is as follows: 0.27 moles of dodecyl amine, 9.09 moles of ethanol and 29.6 moles of deionized water were mixed together to which 1 mole of alkoxide was added under vigorous stirring. After the addition of alkoxide, the reaction mixture was stirred for 1/2 hours and then kept aside at room temperature in the range of 19–35 hours. After this aging reaction, the sample was transferred to a glass plate and air-dried. The neutral template was removed from the air-dried materials in two ways: (a) by repeated washing with hot ethanol and finally the samples were dried at 80°C in an oven and (b) by heating at 300°C for 4 hours in a furnace.

All the synthetic samples were characterized by powder X-ray diffraction (XRD) using Scintag diffractometer with Ni-filtered CuKα radiation. Adsorption and desorption isotherms of N_2 were measured from which surface area and pore-size distribution were determined. Pore-size distribution was calculated using the BJH method [17]. The N_2 isotherms were measured by using an Autosorb-1 apparatus. Water adsorption and desorption isotherms were determined by a volumetric method using an automated device [18] after degassing at 25°C or 200°C. The pressure was recorded by a high-accuracy pressure transducer. The equilibrium conditions were defined by the pressure difference of 0.05 Torr during a period of at least 4 minutes. These conditions were found to be adequate as verified by the published results on aluminosilicate zeolites.

3. Results and Discussion

Powder XRD analyses, BET N_2 surface areas, pore-size distributions and amounts of water adsorbed of the various synthetic mesoporous materials are given in Table 1. The silica mesoporous materials synthesized by two different techniques show similar d spacings and pore-size distributions with very high surface areas as has been reported previously by others [2, 3, 8]. The N_2 adsorption-desorption isotherms of the two Si mesoporous samples are presented in Figs. 1 and 2 which show well-defined steps between partial pressures, P/P_0 of 0.25 to 0.45. These steps, during

Table 1. Powder XRD analyses, BET N_2 surface areas, pore-size distributions and amounts of water adsorbed of synthetic mesoporous materials.

Characterization and measured properties	Cationic template	Mesoporous material composition using neutral template of dodecyl amine				
	Si	Si	Al	Ti	Zr	Nb
X-ray diffraction						
As prepared	3.7 nm	3.67 nm	No clear peak	2.93 nm	~3 nm*	~3 nm
After Ethanol wash	—	3.68 nm	—	2.94 nm	—	3.6 nm*
After 300°C/4 h[#]	3.9 nm**	4.5 nm	No clear peak	3.39 nm	~3 nm*; 0.295 nm; 0.182 nm	3.39 nm
BET N_2 surface areas						
After ethanol wash	—	1072 m²/g	395 m²/g	204 m²/g	393 m²/g	11 m²/g
After 300°C/4 h	956 m²/g**	826 m²/g	407 m²/g	258 m²/g	178 m²/g	77 m²/g
Pore-size, diameter						
After ethanol wash	—	~2.4 nm	~6 nm	~3.8 nm*	1.8 nm; 3.5 nm*	~3.8 nm
After 300°C/4 h	~2.9 nm**	~2.9 nm	~6 nm	~3.8 nm*	~3.8 nm*	~3.8 nm
Amounts of water adsorbed						
After ethanol wash	—	59.9%	70.1%	11.7%	20.4%	10.2%
After 300°C/4 h	93.4%**[†]	75.4%[$]	58.0%[$]	14.8%[$]	10.8%[$]	9.7%[$]

*Small peak; **300°C/25 hours; [†]degassed at 200°C; [$]degassed at 25°C; [#]the increase in *d* spacings of samples after calcination at 300°C, compared to as prepared- or ethanol-washed ones, cannot be unequivocally explained at this stage.
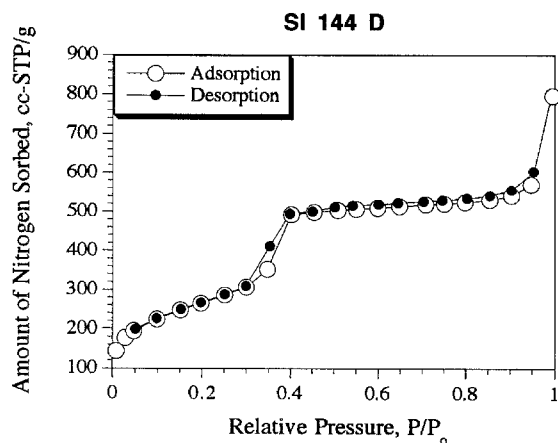

SI 144 D

Figure 1. N_2 adsorption-desorption isotherms of a mesoporous silica prepared by using a cationic template (2, 3) and calcined at 300°C/25 hours.

HMS EB

Figure 2. N_2 adsorption-desorption isotherms of a mesoporous silica prepared by the neutral template method (8, 9) and calcined at 300°C/4 hours.

adsorption, are due to the filling of mesopores in the framework or intraparticle porosity. These samples also show a second step above partial pressures P/P_0 of 0.9 which corresponds to the interparticle porosity. Both the mesoporous silicas show sharp pore-size
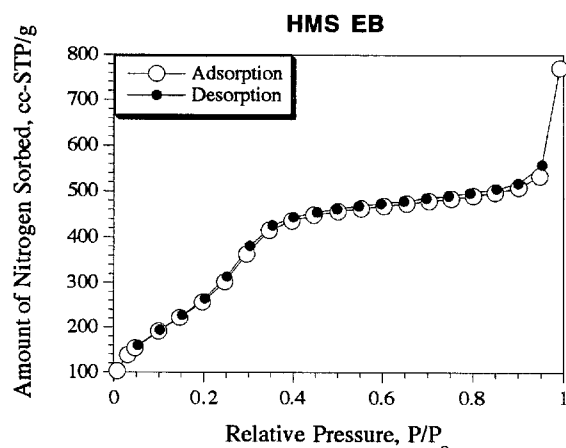
distribution at about 2.9 nm (Figs. 3 and 4). Figure 5 shows a transmission electron micrograph of the mesoporous silica sample which was prepared by the neutral template route [8] and heated at 300°C for 4 hours. The micrograph shows agglomerates of
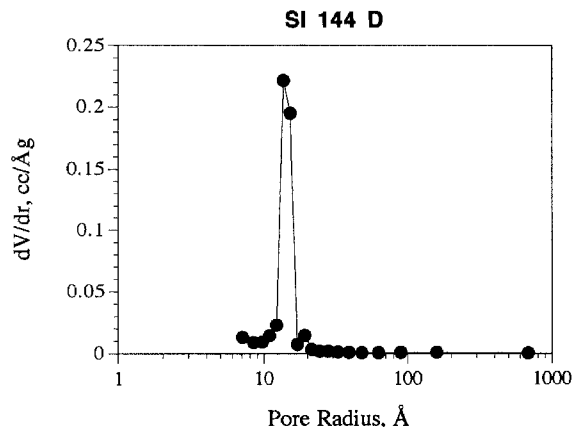
SI 144 D

Figure 3. Pore-size distribution of mesoporous silica prepared by using the cationic template and calcined at 300°C/25 hours.
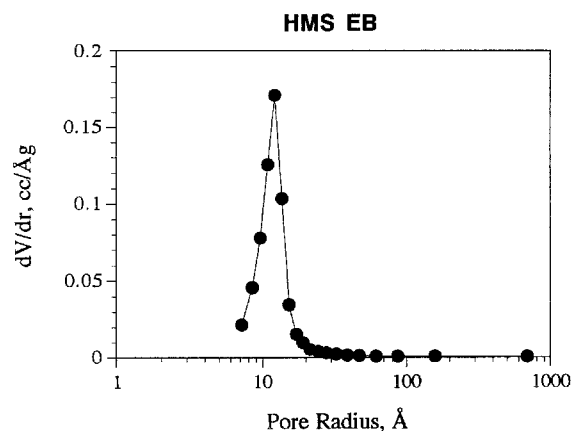
HMS EB

Figure 4. Pore-size distribution of mesoporous silica prepared by the neutral template method and calcined at 300°C/4 hours.

rounded particles with low-density regions corresponding to pores (Fig. 5). The sample shows no crystallinity by electron diffraction.

The water adsorption-desorption isotherms of both the mesoporous silicas are presented in Figs. 6 and 7. The adsorption isotherms are of Brunaur Type V mesoporous (weak interaction) [19] with very little adsorption until a P/P_0 of about 0.45 (Fig. 7) and 0.55 (Fig. 6) followed by a sudden vertical rise in adsorption. The lack of significant adsorption until a P/P_0 of about 0.45 or 0.55 is due to the weakly polar or nonpolar (hydrophobic) nature of the silica surface. The steep rise in adsorption between a P/P_0 range of 0.45 to 0.7 is due to the volume filling of mesopores. These types of unusual water adsorption-desorption isotherms have been reported by us previously for

synthetic aluminophosphate and silicoaluminophosphate molecular sieves [20, 21]. Our previous results with the above microporous materials showed that the P/P_0 at which a steep rise in adsorption takes place is a function of the pore size, i.e., the smaller the pore-size, the lower the P/P_0 where the pore filling takes place. The results presented here with the mesoporous silicas confirm the above finding. The above property of the silica mesoporous molecular sieves which results in sudden mesopore filling in the P/P_0 range of 0.45 to 0.55 can be used in the design and fabrication of humidity sensors. The amounts of condensation at P/P_0 greater than 0.7 (Figs. 6 and 7) are small which suggests that the interparticle porosity is small compared to the intraparticle mesoporosity. Both the mesoporous silica samples exhibited hystereses which extended to very low pressures in one case (Fig. 6). The hysteresis at low pressures in this case is possibly because of the chemical reaction of water with silica surfaces, and this water could not be removed during desorption at 25°C. It should also be noted that this sample (Fig. 6) was degassed at 200°C while the other sample (Fig. 7) was degassed at 25°C (Table 1). The mesoporous silica samples adsorbed 75.4 and 93.4% of water which suggests that the total pore volume available is very high as has been shown with the hydrocarbon sorption measurements [3]. The water adsorption-desorption isotherms of mesoporous silica materials are reproducible with repeated cycles which suggests that these materials are very stable and can be used in the design and fabrication of humidity sensors.

The mesoporous alumina sample prepared by the neutral template route did not show any clear peak by XRD (Table 1). Electron diffraction, however, showed bands at 6.2 Å, 3.2 Å, 2.45 Å, 1.81 Å, 1.45 Å, 1.32 Å, 1.13 Å, etc. which matched somewhat with boehmite. Transmission electron micrograph (Fig. 8) shows a fibrillar morphology. The N_2 adsorption-desorption isotherms show a Type IV adsorption isotherm (Fig. 9) with only one hysteresis loop between a P/P_0 range of 0.55 to 0.9. The pore-size distribution is somewhat sharp and centered at about 6 nm (Fig. 10). This mesoporous material showed a very high surface area of 407 m^2/g (Table 1). Water adsorption-desorption isotherms of the alumina mesoporous material are presented in Fig. 11. These isotherms are of Type IV with a somewhat hydrophilic nature of the surface. The mesopores are filled with water between a P/P_0 range of 0.55–0.9. No distinction between the framework-confined and interparticle pores can be seen probably
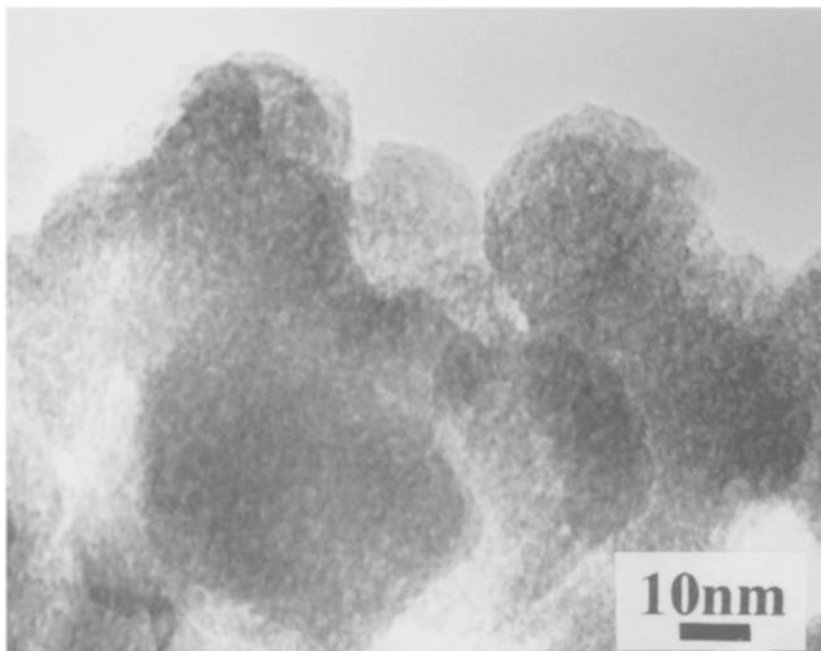
Figure 5. Transmission electron micrograph of mesoporous silica prepared by the neutral template method and calcined at 300°C/4 hours.
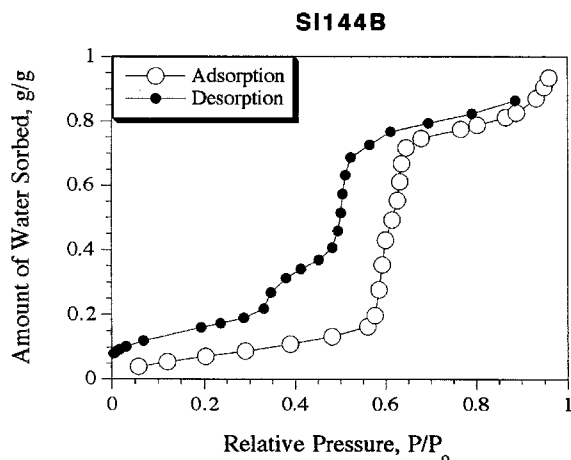

Figure 6. Water adsorption-desorption isotherms of mesoporous silica prepared by the cationic template method and calcined at 300°C/25 hours.
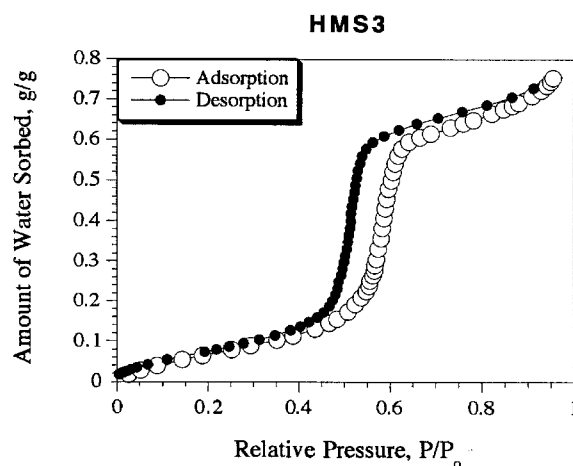
Figure 7. Water adsorption-desorption isotherms of mesoporous silica prepared by neutral template method and calcined at 300°C/4 hours.

because the size range of the two types of pores overlap. It is interesting to note that the N_2 and H_2O adsorption-desorption isotherms are very similar with the alumina mesoporous material unlike the silica mesoporous materials described above.

Mesoporous materials of Ti, Zr, and Nb oxide compositions prepared by the neutral templating route do

not exhibit N_2 adsorption-desorption isotherms which are typical of Si mesoporous materials with two steps (Figs. 1 and 2) or of Al mesoporous material (Fig. 9). The N_2 adsorption-desorption isotherms appear to be Type I. The pore-size distribution data show only small peaks in the mesopore region (Table 1) although these samples show XRD peaks around 3 nm. The water
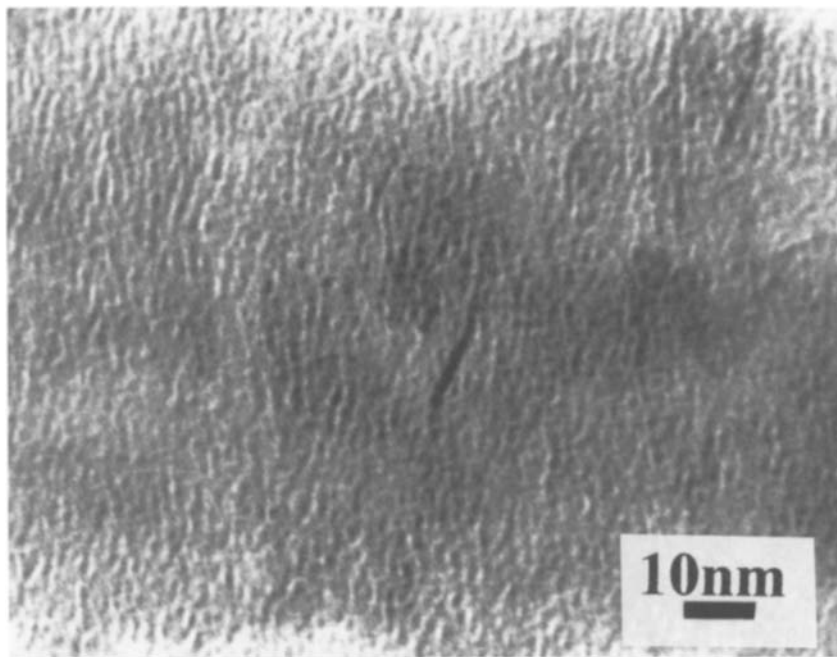
Figure 8.   Transmission electron micrograph of mesoporous alumina by neutral template route and calcined at 300°C/4 hours.
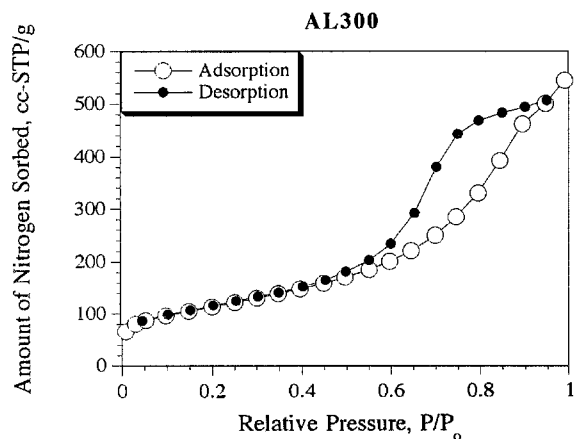

Figure 9. N_2 adsorption-desorption isotherms of a mesoporous alumina prepared by the neutral template route and calcined at 300°C/4 hours.
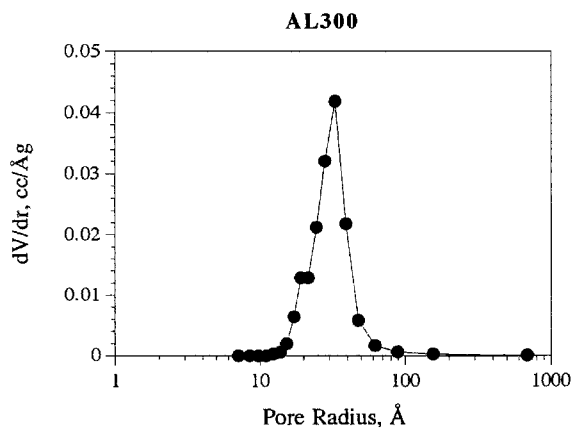

Figure 10.   Pore-size distribution of mesoporous alumina prepared by the neutral template route and calcined at 300°C/4 hours.

adsorption-desorption isotherms are of moderate Type I revealing the hydrophilic nature of these samples. Water adsorption-desorption isotherms of titania, zirconia and niobia porous materials are shown in Figs. 12, 13 and 14, respectively. The surface areas and pore volumes as revealed by N_2 and H_2O adsorptions, respectively, (Table 1) are low compared to the silica and alumina mesoporous materials described above. Thus, these materials of Ti, Zr, and Nb oxide compositions do not appear to be truly mesoporous unlike the Si and Al oxide materials. The Ti oxide material is stable up to 300°C but transforms to very fine anatase at 350°C. The Zr oxide material transforms to poorly crystalline tetragonal ZrO_2 at 300°C while the Nb oxide material remains amorphous at 300°C.
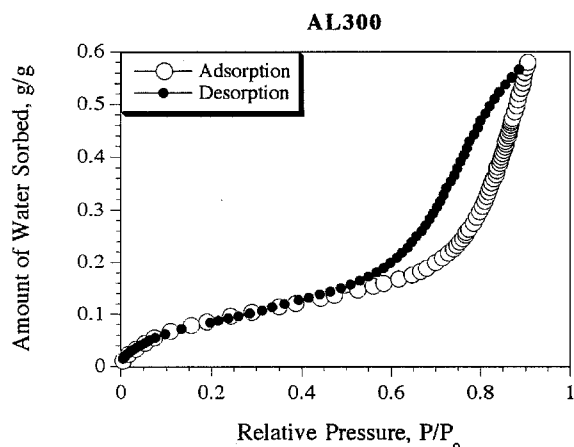
Figure 11. Water adsorption-desorption isotherms of mesoporous alumina by the neutral template route and calcined at 300°C/4 hours.
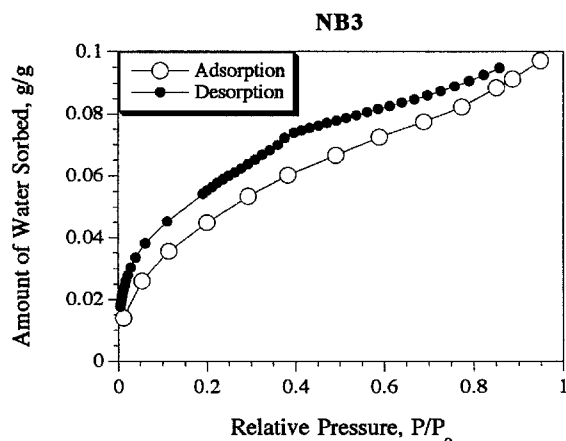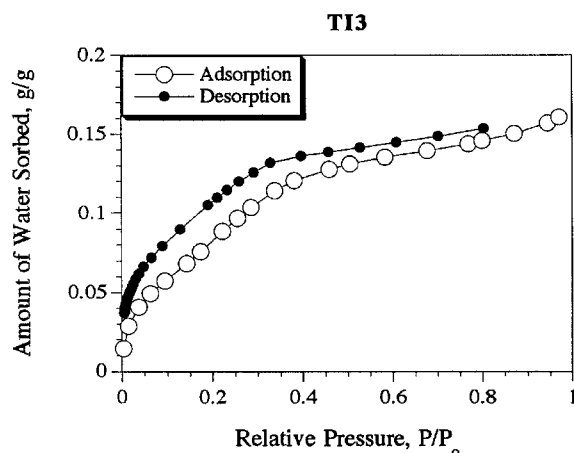

Figure 12. Water adsorption-desorption isotherms of porous titania prepared by the neutral template route and calcined at 300°C/4 hours.

Figure 13. Water adsorption isotherm of porous zirconia prepared by the neutral template route and calcined at 300°C/4 hours.

Figure 14. Water adsorption-desorption isotherms of porous niobia prepared by the neutral template route and calcined at 300°C/4 hours.
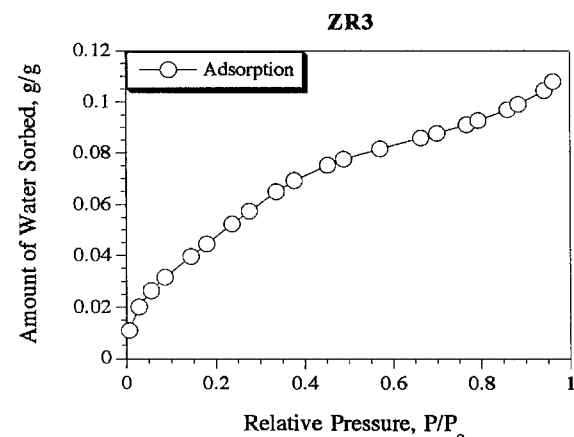
4. Conclusions

Mesoporous silica and alumina molecular sieves exhibit Type V and Type IV water adsorption isotherms, respectively. Their water adsorption-desorption isotherms show well-defined hysteresis loops at high P/P_0 corresponding to the mesopores. Titania, zirconia, and niobia porous materials prepared by the neutral template route show Type I water adsorption isotherms which indicates that they are mostly microporous.

Acknowledgments

References

1. T. Yanagisawa, T. Shimizu, K. Kuroda, and C. Kato, Bull. Chem. Soc. Jpn. 63, 988 (1990).
2. C.T. Kresge, M.E. Lenowicz, W.J. Roth, J.C. Vartuli, and J.S. Beck, Nature 359, 710 (1992).
3. J.S. Beck, J.C. Vartuli, W.J. Roth, M.E. Leonowicz, C.T. Kresge, K.D. Schmitt, C.T.W. Chu, D.H. Olson, E.W. Sheppard, S.B. McCullen, J.B. Higgins, and J.L. Schlenker, J. Am. Chem. Soc. 114, 10834 (1992).
4. A. Monnier, F. Schuth, Q. Huo, D. Kumar, D. Margolese, R.S. Maxwell, G.D. Stucky, M. Krishnamurthy, P. Petroff, A. Firouzi, M. Janicke, and B.F. Chemelka, Science 261, 1299 (1993).
5. Q. Huo, D.I. Margolese, U. Ciesla, P. Feng, T.E. Gier, P. Sieger, R. Leon, P.M. Petroff, F. Schuth, and G.D. Stucky, Nature 368, 317 (1994).
6. A. Firouzi, D. Kumar, L.M. Bull, T. Besier, P. Sieger, Q. Huo, S.A. Walker, J.A. Zasadzinski, C. Glinka, J. Nicol, D.

Margolese, G.D. Stucky, and B.F. Chemelka, Science **267**, 1138 (1994).

7. Q. Huo, R. Leon, P.M. Petroff, and G.D. Stucky, Science **268**, 1324 (1995).

8. P.T. Tanev and T.J. Pinnavaia, Science **267**, 865 (1995).

9. P.T. Tanev and T.J. Pinnavaia, in *Advances in Porous Materials*, edited by S. Komarneni, D.M. Smith, and J.S. Beck, Mat. Res. Soc. Symp. Proc. (Pittsburgh, PA, 1995), vol. 371, p. 63.

10. S.A. Bagshaw, E. Prouzet, and T.J. Pinnavaia, Science **269**, 1242 (1995).

11. K.M. Reddy, I. Moudrakovski, and A. Sayari, J. Chem. Soc. Chem. Commun. **1059** (1994).

12. A. Corma, M.T. Navarro, and J. Pérez Pariente, J. Chem. Soc. Chem. Commun. **147** (1994).

13. P.T. Tanev, M. Chibwe, and T.J. Pinnavaia, Nature **368**, 321 (1994).

14. C.-Y. Chen, H.-X. Li, and M.E. Davis, Microporous Mater. **2**, 17 (1993).

15. P.J. Branton, P.G. Hall, M. Treguer, and K.S.W. Sing, J. Chem. Soc. Faraday Trans. **91**, 2041 (1995).

16. P. Llewellyn, F. Schuth, Y. Grillet, F. Rouquerol, J. Rouquerol, and K.K. Unger, Langmuir **11**, 574 (1995).

17. E.P. Barrett, L.G. Joyner, and P.P. Halenda, J. Am. Chem. Soc. **73**, 373 (1951).

18. S. Yamanaka and S. Komarneni, U.S. Patent 5,058,442, Oct. 22 (1991).

19. K.S.W. Sing, D.H. Everett, R.A.W. Haul, L. Moscou, R.A. Pierotti, J. Rouquerol, and T. Siemieniewska, Pure and Appl. Chem. **57**, 603 (1985).

20. P.B. Malla and S. Komarneni, Mat. Res. Soc. Symp. Proc. **233**, 237 (1991).

21. P.B. Malla and S. Komarneni, Zeolites **15**, 324 (1995).